Numerical modelling of the turbine Power Take Off for the UGEN floating Wave Energy Converter

L. Pietra[1], N. Fonseca[1] and J. Pessoa[1]

[1] Centre for Marine Technology and Engineering,
Instituto Superior Técnico,
Av. Rovisco Pais 1, Lisbon, Portugal
E-mail: luca.pietra@mar.ist.utl.pt

Abstract

UGEN is a floating OWC, enclosing a U-tank with chambers connected through a duct hosting an air turbine. A frequency-domain model of the body's dynamics had been developed, representing the turbine as a linear damping. The scope of this work is to develop a more accurate model of the turbine. An impulse and a Wells turbine are considered. Time-domain models are built in SIMULINK, giving special attention to variations of air density, whose compressibility influences the turbine's performance and the whole WEC's dynamics. Harmonic and irregular waves are tested, for validation and simulation respectively, with forced oscillation of the water columns; the optimal combination of diameter and speed is sought for each of the two turbines. Instantaneous and average power and efficiency are evaluated.

Keywords: air turbine, oscillating water column, time-domain simulation

1. Introduction

The UGEN (U-tank Generator) concept, a floating WEC based on the principle of the Oscillating Water Column (OWC), was proposed in [1-2]: it has the peculiarity of having two chambers instead of one, connected on the bottom part through an internal water tank and on the top through a duct hosting the air turbine; the chambers are not open to the sea and atmosphere, but enclosed in the floater's body. With the floater's rolling movement, the two chambers play for each other the role of low-pressure discharge reservoir. Fig. 1 shows a schematic of the UGEN internal tank layout.

A frequency domain numerical model was developed [1] to investigate the system dynamics; in addition to the six degrees of freedom (d.o.f.) of the floating body, a seventh coupled rotational d.o.f. (x_7 in Fig. 1) was used to represent the movement of the water columns; the presence of the air turbine in the top duct was represented by a linearized damping coefficient acting on such d.o.f.. The average absorbed power was calculated making use of such coefficient (B_{PTO}) and the damping moment it induces (M_{PTO}), multiplied by the relative roll velocity $\dot{\theta} = (\dot{x}_7 - \dot{x}_4)$

$$\overline{P} = M_{PTO} \cdot \dot{\theta}(t) = B_{PTO} \cdot \dot{\theta}^2\,(t) \qquad (1)$$

An experimental campaign with a 1:16 scale model in regular and irregular waves was carried out [2], where the damping given by the turbine was represented by a grid in the model's duct.

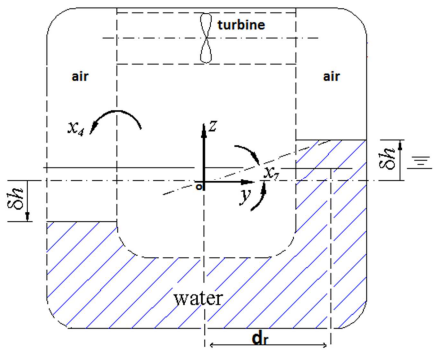

Figure 1: side view of the U-GEN double internal OWC chamber. The shape of the floater is not yet fully optimized. x_4 is the tank's roll movement, x_7 the roll angle of the internal body of water, δh the displacement of its free surface and d_r the distance between G and the center of the water column.

The frequency-domain model was improved in [3] by introducing one more equation representing the turbine's behavior, derived from the flow-pressure relationship (characteristic curve), thus accounting for air compressibility, neglected in the previous model. Such equation was derived assuming small amplitude motions of the columns and a linearized isentropic relation for the air discharge between the chambers [4].

The objective of the present work is to further enhance the model by introducing a detailed and correct representation of the turbine and air chamber dynamics and, thanks to the time-domain approach,

include nonlinearities in the turbine behavior and, in further work, control strategies of the Power Take Off (PTO). The model developed will be applied to optimize WEC's components and working conditions.

1.1 State of the art of air turbines

Early prototypes OWCs adopted unidirectional air turbines with valves or flaps to rectify the air flow. From the late 70s, several self-rectifying turbines were proposed; among these, the Wells gained most recognition and since then most OWCs made use of it. More recently, the bi-directional impulse turbine was introduced, overcoming some drawbacks of the Wells; each comes in a set of possible arrangements (single or double wheel, with or without guide vanes, fixed or variable ducts).

The rotor blades of a Wells turbine have symmetric airfoil profile, with the chord lying on its plane of rotation. Of simple and economical construction, the Wells turbine has inherent disadvantages: narrow range of flow rates with useful efficiency, poor starting characteristics, high speed [5]. Its rotor has an inherent limit due to its blade shape, stalling for angles of incidence above 13 degrees [6]. This implies an upper limit to the flow (at given speed) or the use of release or throttle valves. Alternatively, variable-pitch rotor blades can be adopted. Wells turbines have a linear characteristic (or damping) curve, relating the pressure difference to the air flow through a constant K. Valves or pitching blades introduce nonlinear parts in it.

The self-rectifying impulse rotor improves on the Wells, having no stall limit (thus requiring no valves), wider operational range, better efficiency at high flows, lower speeds and good starting characteristics; smaller machines are needed for comparable rated power. The blades are symmetric with respect to the rotor's plane of rotation, but their profile is not symmetrical. A row or static guide vanes is needed on each side of the rotor, either fixed or adjustable (or self-pitching).

Manufacturing is cheaper for the simpler and less numerous blades of a Wells (given a diameter), and idling drag losses are minimal with this kind of turbine.

1.2 State of the art of numerical models

Models of the turbine (generator) have been developed and used by a number of authors [4-10]. Frequency-domain models are used for optimization purposes in order to run fast simulations of different arrangements, whereas time domain models give a precise representation of the working of a specific machine, for a precise evaluation of its performance.

In some cases [4-8] the power module is integrated in the whole OWC machine model; in others [9-10], the model of the turbine (and generator/gearbox) is self-standing and separate from the rest of the OWC device.

2. Basic model

In [3], the system of dynamic equations of the UGEN floater was solved, coupled to one extra equation for the added degree of freedom (oscillation of water in internal tank, x_7) and one for the Wells turbine, with the pressure difference between the chambers as unknown. Fig. 2 shows the transfer function thus calculated, for the relative roll velocity ($\dot{x}_7 - \dot{x}_4$).

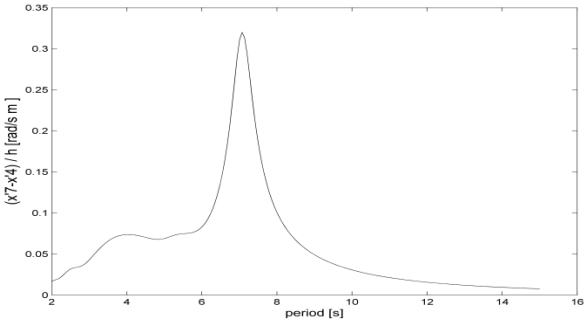

Figure 2: transfer function for relative roll velocity between the tank and the internal mass of water

The scope of the present work is to refine the representation of the Power Take Off by allowing the simulation of other turbines, specifically the self-rectifying impulse. Due to the non-linearity of its characteristic curve, the simulation has to be in the time domain (allowing simulating the system's behavior in irregular sea states); based on examples from literature [9-10], a SIMULINK model is chosen, shown in Fig. 3.

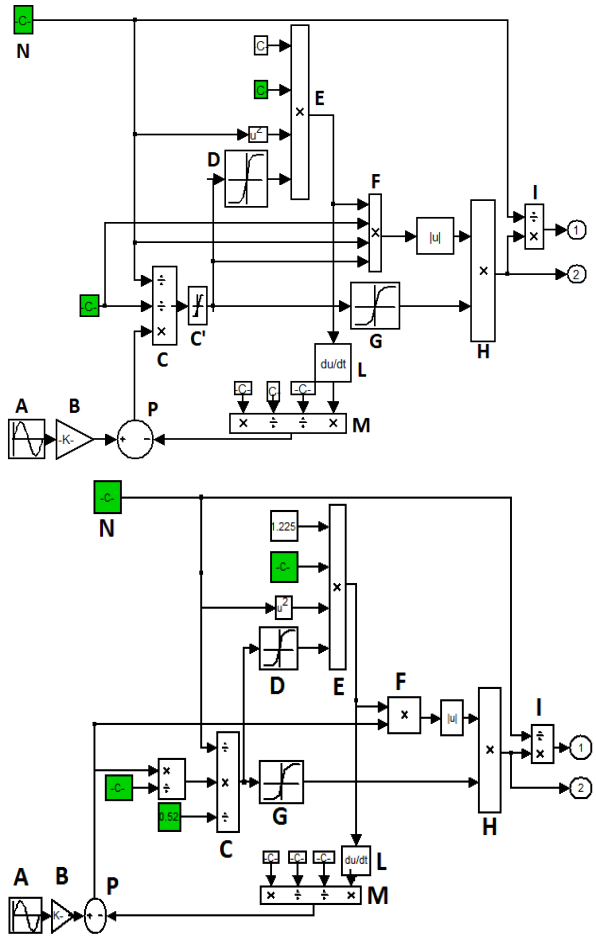

Figure 3: the SIMULINK models used to represent the turbines in U-GEN (shown with regular wave input) a) Wells turbine b) self-rectifying impulse turbine

The green boxes include elements that change with turbine size (diameter, mean radius, passage area) and the rotational speed (N). The two schemes for a Wells and an impulse turbine differ slightly due to the different definitions of the non-dimensional parameters in [4] and [11], respectively, whose curves were used.

The input (A) is the relative roll velocity $(\dot{x}_7 - \dot{x}_4)$ between the water column and the floater: the picture shows the regular waves setup, with a sinusoid of desired frequency and amplitude; for irregular waves, the input comes from the MATLAB routine calculating the wave elevation in time domain (see section 4).

Assuming $(\dot{x}_7 - \dot{x}_4)$ to be small, the expression for $\dot{h}$, the vertical velocity of the columns, is linearized (angles instead of their tangents, as in (2)). The air volume flow Q is calculated (B) by multiplying the input (A) by the column area A_{tk} (taken twice according to Fonseca and Pessoa [3]) and the roll radius d_r, i.e. distance between G and the center of the column:

$$Q = 2A_{tk}\dot{h} = 2A_{tk}d_r(\dot{x}_7 - \dot{x}_4) \tag{2}$$

The air volume flow is used to calculate the non-dimensional flow coefficient (C), respectively as

$$\Phi = \frac{Q}{ND^3} \tag{3}$$

for the Wells [4], and

$$\varphi = \frac{v_x}{u_r} = \frac{\frac{Q}{A_T}}{Nr_r} \tag{4}$$

for the impulse turbine [11], with N rotational speed in rad/s, D outer diameter, v_x air axial velocity, u_r blade tangential speed at mid radius r_r, and A_T passage area. This difference is only due to different definitions used by the authors of the papers where the curves are taken from, but can be converted one into the other.

In the case of the Wells turbine, C' represents the valve that limits the value of the flux to a maximum critical value, above which stall occurs with loss of efficiency. Through the curves from the cited articles, the non-dimensional pressure coefficient Ψ is derived (D) and from it the pressure drop calculated (E) as

$$\Delta p = \Psi \rho D^2 N^2 \tag{5}$$

The derivative of the pressure drop is calculated (L) and multiplied by $V_0/(c_a^2\rho_a)$ to feed the loop (C,D,E,L,M,P) implementing the expression by Falcão and Rodrigues [12] accounting for air compressibility (see section 4), and calculate (P) the actual air flow through turbine Q_t.

$$Q_t = Q - \frac{V_0}{c_a^2 \rho_a}\frac{dp}{dt} \tag{6}$$

, with V_0 being chamber air volume at rest, c_a speed of sound and ρ_a air density at standard conditions.

The pneumatic power P_P is calculated (F) by multiplying the air flow by the pressure drop, taken always positive:

$$P_P = |Q_T \cdot \Delta p| \tag{7}$$

When multiplied (H) by the turbine's efficiency η_T (also obtained from curves (G), starting from the flow coefficient φ), the pneumatic power P_P gives the turbine shaft power P_T (output (2) in the models), which divided (I) by the shaft rotational speed (N) gives the shaft torque T_T (output (1)).

$$T_T = \frac{P_T}{N} = \frac{P_P \eta_T}{N} \tag{8}$$

Quasi-steady approximation is used, as curves originally obtained under steady flow conditions are used to predict the behavior of the turbine under unsteady flow. Quasi-steady approximation was shown to be valid by a number of authors [13]. The setup of the SIMULINK model will be validated against results of frequency domain calculations [3] for the case of a 2.3m diameter Wells turbine with harmonic input.

The rotational speed N influences both φ, and therefore η_T (with inverse proportionality), and Δp, and therefore P_P. A balance needs to be found between increasing pneumatic power and decreasing turbine efficiency, to get the highest extracted energy; turbine performance will therefore be evaluated at different rotational speeds. Different diameters will also be considered for the two turbines, in order to find for each the best combination, and compare them. Due to available non-dimensional curves, only geometrically similar turbines are considered (hub-to-tip ratio and blade shape): a proper geometrical optimization is not sought at this stage.

Time-variant quantities can be compared in terms of peak or average value, the latter being significant to analyze performance and the former providing information to evaluate extreme conditions. For zero-mean quantities, the average is calculated as rms.

3. Results in regular waves

Fig. 4 shows, in terms of average shaft power at constant rpm, the results relative to an input of regular waves of period 7s and amplitude 0.75m, corresponding to peak period and significant wave height (1.5m) of a representative sea state in the west coast of Portugal.

The air flux is similar for both cases because the column motion is imposed, therefore the comparison here is between the two turbines under similar forced flow conditions, rather than between the two setups of the whole machine under similar waves conditions.

Each line in the graph corresponds to a rotor diameter: simulations were run for diameters between 0.5m and 2.5m and rotational speeds between 30 rad/s and 250 rad/s, although only the most significant results are reported in figure. Results from the 2.3m Wells agree with the ones from the frequency-domain model [3], thus validating the present approach.

Average and peak power are not always related: periods of turbine η_T=0 occur, due to low φ; for this, zero-average power conditions can be observed at high rotational speeds, in particular with bigger diameters.

The condition proposed by Falcão and Rodrigues [12] is applied, to prevent sonic effects when the blade/air relative velocity reaches high values:

$$ND < 380 \text{ m/s} \quad (9)$$

(N rotational speed [rad/s], D external blade diameter)

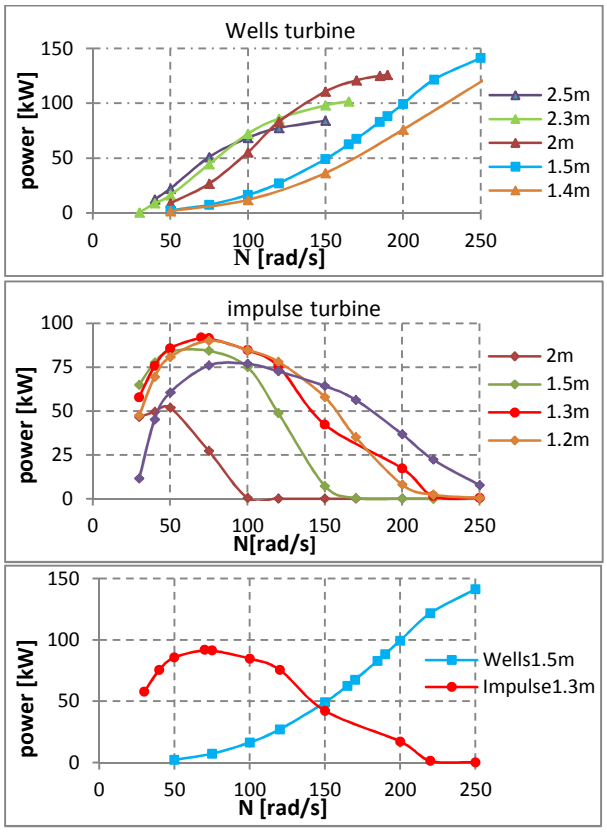

Figure 4: average turbine power in harmonic 7s, 0.75m waves for turbines of different diameters a) Wells b) impulse 0.6 H/T c) chosen Wells vs chosen impulse

Some general observations can be made: smaller impulse turbines perform better at lower rotational speeds, with a more flat curve (little loss in performance when out of optimal regime), while Wells are bigger and give best performance at high rotational speeds, with more loss of performance at non-optimal conditions. Impulse turbines with bigger rotors (rotating at lower rpm) have low average power mostly due to low φ (axial air velocity) and therefore η_T.

It is to be kept in mind that a bigger rotor implies higher material costs, and a higher rotational speed causes more mechanical stress and noise. The Wells requires release valves (in each direction), setting a challenge to find an arrangement in this specific case.

For all these reasons, although the Wells shows higher average power in harmonic waves, there are reasons not to discard the impulse option; a comparison in irregular waves will give a more significant insight: it is chosen to further investigate the setups giving highest average power: 1.5 m Wells and 1.3 m impulse.

Fig. 5 shows the time-domain development of air volume flow, pressure drop and shaft power for these two cases (Fig. 4c) in harmonic 7s, 0.75m waves.

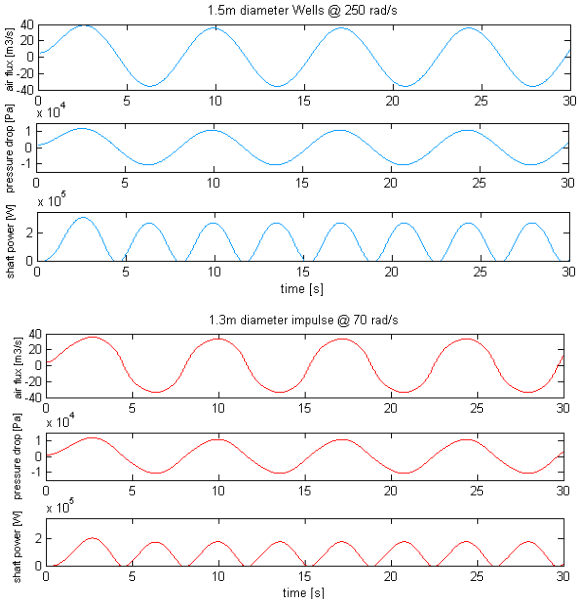

Figure 5: air volume flow, pressure drop and shaft power in harmonic 7s, 0.75m waves
a) 1.5m Wells @350 rad/s b) 1.3m impulse @70 rad/s

4. Results in irregular waves

After validation in harmonic waves, performance in irregular sea states is evaluated: a JONSWAP spectrum with H_s=1.5m, T_P=7s and γ=3.3 is chosen as representative of the climate of Portugal's west coast. The relative roll velocity complex transfer function is calculated from the frequency domain results; from it, the complex response spectrum:

$$S_{response}(\omega) = |\dot{x}_4(\omega) - \dot{x}_7(\omega)|^2 \cdot S_{wave}(\omega) \quad (10)$$

, the squared term being the complex transfer function and S_{wave} the complex wave spectrum; $S_{response}$, through an inverse Fourier transform, gives the relative roll velocity time series used to calculate the air flow (2).

Over 30 minutes (duration defined through convergence tests of average power), the simulated flow has an average of 16.5 m^3/s; this value is referred to the flow called Q (2), while Q_T (6) is different for each case tested, due to the effect of diameter and rotational speed on compressibility effects, through the pressure derivative, as shown by (6).

The chosen diameter for each turbine (Fig. 4c) is used to run simulations: the results are shown in Fig. 6 as average shaft power against rotational speed.

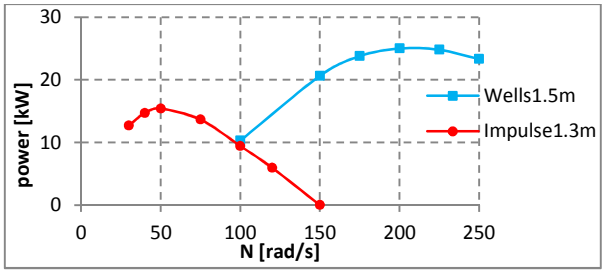

Figure 6: average turbine power in real sea state (JONSWAP 7s, 1.5m) for a Wells and an impulse turbine

Highest average power happens for both turbines at slightly lower rotational speeds than in the harmonic case. Again the Wells outperforms the impulse turbine, with an average shaft power of 25 kW against 16 kW: a difference of 35% that is about the same as in the harmonic case presented in section 2.

A control algorithm to optimize the rotational speed with variations in the time scale of the wave groups would help improving the conversion efficiency.

It would be useful to run simulations with different sea states, to evaluate the yearly energy production of a machine in a specific location.

Fig. 7 shows the time history of wave elevation, air flux, pressure drop and shaft power for the two turbines. The shaft power is always positive (or zero). The two cases show similar trends everywhere but in the last graph, relative to shaft power, where the Wells shows better efficiency in low flow coefficients, while the impulse in high ones; the impulse turbine shows a less sharp trend of the power output.

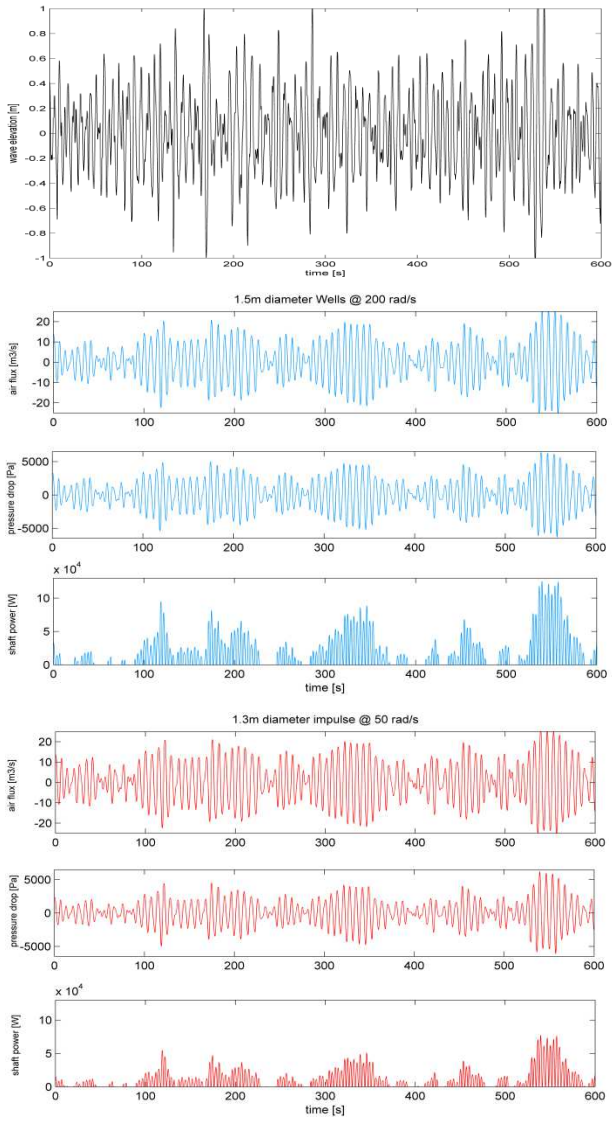

Figure 7: wave elevation, air flux, pressure drop and turbine shaft power in irregular waves a)1.5m Wells turbine @200 rad/s b)1.3m impulse turbine @50 rad/s

5. Compressibility

Air density variations in an OWC are not negligible and get more significant the bigger the volume [4]. Some authors analyzed the phenomenon and proposed analytical ways to represent it [12-14]. Equation (6) is a rearrangement of the linearized expression proposed in [12], for small ρ and V variations and isentropic expansion/compression. The "loop" in the SIMULINK model (C,D,E,L,M,P in Fig. 3) implements its solution. In this section the differences between models with and without the "compressibility loop" are investigated.

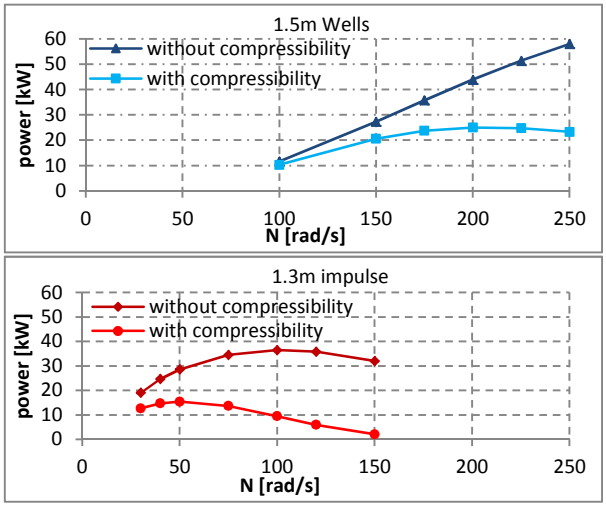

Figure 8: average shaft power with and without compressibility effects included a) 1.5m Wells turbine b)1.3m impulse turbine

Fig. 8 shows how the compressibility effects get more important at higher rotational speeds; simulations run but not represented here show that these effects are stronger for smaller diameter rotors; both tendencies affect more impulse turbines and might be due in both cases to air passage made more difficult, either by faster moving blades or reduced passage area.

Fig. 9 shows time-domain plots of air volume flow, pressure drop and shaft power with and without compressibility accounted, highlighting its effect: all quantities are reduced when compressibility is included and a phase shift is introduced (spring effect). With the Wells turbine, at optimal rotational speed (200 rad/s) the loss in average power is 43%, getting more significant at higher speeds (60% at 250 rad/s) and negligible at lower (100 rad/s). Without compressibility, the average power increases with rotational speed, until occurrence of sonic effects. For the impulse turbine, the optimal speed is 50 rad/s and average power loss due to compressibility is 66%. With no compressibility, the power-rotational speed curve keeps a similar shape (Fig. 8b) but the optimal speed is 100 rad/s. Losses increase at higher rotational speeds, and are negligible at lower ones (20 rad/s).

At all rpm and regardless whether compressibility is accounted for, the pressure drop is higher across the impulse turbine, which could be why the effects of air compressibility are more significant for it.

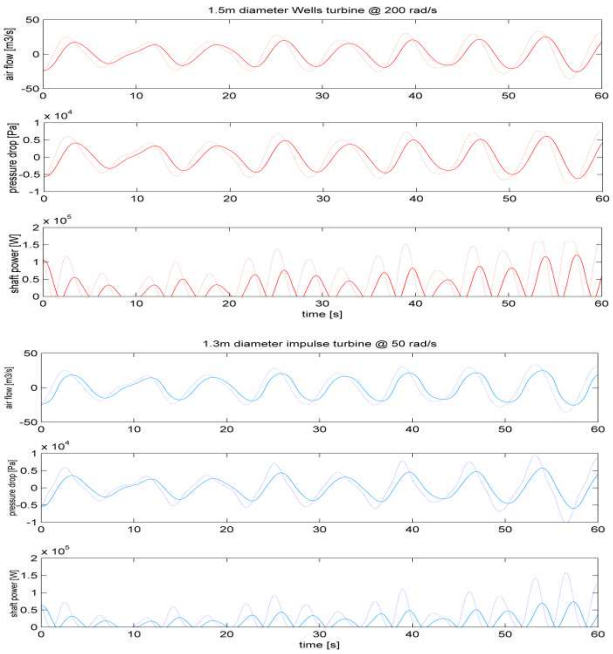

Figure 9: air flux, pressure drop and shaft power with (solid line) and without (dotted line) compressibility effects a) 1.5m Wells turbine @ 200rad/s b)1.3m impulse turbine @ 50 rad/s.

6. Conclusions and future work

A time-domain SIMULINK model was implemented to improve the representation of the turbine in the UGEN floating WEC. A Wells and an impulse turbine were simulated, using as input the relative roll velocity and using published characteristic curves to calculate air flux, pneumatic and shaft power, efficiency and torque. The model was validated in harmonic waves and used to compare the two turbines in an irregular sea state representative of Portugal west coast; for each, the best combination of diameter and rotational speed was found. As expected, the impulse turbine performs best at lower rpm and with smaller diameter than the Wells. Nonetheless, the latter gives better results in terms of average power for the given sea state. The Wells setup includes valves, introducing complexity and cost in building and O&M; also, higher rotational speed and bigger diameter cause more severe mechanical stresses. Therefore the outcome of the confrontation is not trivial, especially if an impulse turbine with linked guide vanes were considered, improving on efficiency although introducing mechanical complexity.

The effect of air compressibility was studied and found to be more significant than expected, and stronger in the case of the impulse turbine.

This work was based on transfer functions calculated using a system of frequency domain equations that include a Wells turbine [3]. The influence of a different turbine on the floater's and water column's dynamics is not accounted for: this is the main improvement to implement, by including a different turbine relation within the pressure equation; the ultimate improvement will be to express the whole body-tank-PTO coupled dynamics in the time domain.

Generator and gearbox need to be included and a control system implemented to optimize the rotational speed, adapting it to instantaneous wave conditions.

Acknowledgements

This work has been financed and was performed in the scope of the project "Design of mooring systems for floating wave energy converters", financed by Fundação para a Ciência e a Tecnologia (FCT) under contract PTDC/EME-MFE/103524/2008.

References

[1] N. Fonseca, N.R. Silva, J. Pessoa. (2001): Numerical modeling and assessment of the UGEN floating wave energy converter. International Journal of Maritime Engineering - 153 (4), The Royal Inst. of Nav. Arch.

[2] N. Fonseca, J. Pessoa, N.R. Silva, M. Le Boulluec, J. Ohana (2010): Model tests of a wave energy converter based on water oscillating in a U tank. 12èmes Journées de l'Hydrodynamique. Nantes, France.

[3] N. Fonseca, J. Pessoa. (to be published): Numerical modeling of Wave Energy Converter based on U-shaped interior oscillating water column.

[4] A.F.O. Falcão, P.A.P. Justino (1999): OWC wave energy devices with air flow control. Ocean Engineering Vol. 26. Pp 1275-1295.

[5] T. Setoguchi et al. (2001): A review of impulse turbines for wave energy conversion. Renewable Energy Vol. 23. Pp 261–292.

[6] S. Salter (1993): Variable Pitch Air Turbines. Proceedings of European Wave Energy Symposium. Edinburgh, Scotland. Pp 435-442.

[7] V. Jayashakar et al. (2009): A twin unidirectional impulse turbine topology for OWC-based wave energy plants. Renewable Energy Vol. 34 (3). Pp 692-698.

[8] C. Josset, A.H. Clément (2007): A time-domain numerical simulator for oscillating water column wave power plants. Renewable Energy Vol. 32. Pp 1379-1402.

[9] S. Anand et al. (2007): Performance estimation of bi-directional turbines in wave energy plants. Journal of Thermal Science Vol. 16 (4). Pp 346-352.

[10] C.E. Tindall, M. Xu (1996): Optimizing a Wells-turbine-type wave energy system. IEEE Transactions on Energy Conversion Vol. 11 (3). Pp 631-635.

[11] A. Thakker et al. (2002): Application of numerical simulation method to predict the performance of wave energy device with impulse turbine. Journal of Thermal Science Vol. 12 (1). Pp 38-43.

[12] A.F.O. Falcão, R.J.A. Rodrigues (2002): Stochastic modeling of OWC wave power plant performance. Applied Ocean ResearchVol. 24. Pp 59-71.

[13] T. Setoguchi et al. (1996): Impulse turbine with self-pitch-controlled guide vanes connected by links. International Journal of Offshore and Polar Engineering Vol. 6(1). Pp 76–80.